

Supplementary Information

Tuning the electro-catalytic activity of the Zn-Cu MOF/rGO nanocomposite as a novel enzyme-free electrochemical sensor for the detection of Oxytocin hormone

Md Zainul Abedeen¹, Manish Sharma¹, Himmat Singh Kushwaha¹, Ragini Gupta^{1,2,*}

¹Materials Research Centre, Malaviya National Institute of Technology Jaipur, Jaipur 302017, India

²Department of Chemistry, Malaviya National Institute of Technology Jaipur, Jaipur 302017, India

*E-mail: rgupta.chy@mnit.ac.in

Table of content

Text S1. Reagent and Materials

Text S2. Instrumentation

Fig. S1. (a) FE-SEM image of Zn-Cu MOF/rGO, (b) Energy-dispersive spectroscopy (EDS) spectrum of Zn-Cu MOF/rGO, (c) elemental mapping image of copper, (d) elemental mapping image of oxygen, (e) elemental mapping image of carbon, (f) elemental mapping image of zinc, and (d) elemental mapping image of nitrogen.

Fig. S2. FE-SEM image of Zn-Cu MOF

Fig. S3 Interlayer plane of the Zn-Cu MOF/rGO nanocomposite

Fig. S4. Comparative CV of Zn-Cu MOF/rGO-A, Zn-Cu MOF/rGO, and Zn-Cu MOF/rGO-B recorded in the 10 mM $K_3[Fe(CN)_6]/K_4[Fe(CN)_6]$ + 0.1 M KCl at the scan rate of 50 mV/s.

Fig. S5. (a) DPV curve recorded for the bare GCE, Cu MOF, Zn MOF, Cu MOF/rGO, Zn MOF/rGO, Zn-Cu MOF, Zn-Cu MOF/rGO, (b) DPV curve recorded for the rGO modified GCE without and with different concentrations of OXY (Supporting electrolyte: 0.1 M ABS, pH 5).

Fig. S6. DPV response curve for Zn-Cu MOF/rGO/GCE in OXY and other analyte presence (0.1 M ABS, pH 5).

Fig. S7. DPV response curve for Zn-Cu MOF/rGO/GCE in the presence of different analytes, (a) Urea, (b) Ascorbic acid (AA), (c) Fe^{2+} , (d) Glucose, (e) Cl^- , (f) H_2O_2 , (g) Sr^{2+} , (h) Pb^{2+} , (i) Ca^{2+} (0.1 M ABS, pH 5).

Fig. S8. DPV curve for the Zn-Cu MOF/rGO/GCE for the five different electrodes.

Fig. S9. (a) CV curve for the different number of cycles for stability study, (b) corresponding current variation.

Table S1. Parameters for the synthesis of composite material using a one-pot solvothermal approach.

Table S2. Electrochemical properties for the different electrodes.

Table S3: List of the oxidation peak current for the different materials modified on GCE in 0.1 M ABS (pH 5)

Text S1. Reagent and Materials

Copper (II) nitrate trihydrate ($\text{Cu}(\text{NO}_3)_2 \cdot 3\text{H}_2\text{O}$), potassium ferrocyanide trihydrate ($\text{K}_4[\text{Fe}(\text{CN})_6] \cdot 3\text{H}_2\text{O}$), sodium hydroxide (NaOH), sodium phosphate dibasic (Na_2HPO_4), zinc nitrate hexahydrate, sodium acetate, potassium ferricyanide trihydrate ($\text{K}_3[\text{Fe}(\text{CN})_6] \cdot 3\text{H}_2\text{O}$), potassium chloride (KCl), sodium phosphate monobasic (NaH_2PO_4), and benzene dicarboxylic acid (BDC), were purchased from Merck and used without any purification. Ethanol (99.9 %), N, N-dimethyl formamide (DMF) (99.7 %), graphite flakes, sulphuric acid, potassium permanganate, hydrochloric acid, Isopropyl alcohol (99.7 %), and were purchased from Fisher Scientific, and nafion D-521 dispersion 5 % w/w in water as a binder was obtained from Alfa Aesar. Oxytocin injection I.P 10 I.U (8.34 μM) (Pfizer Limited, India) was bought from the medical drug supplier. Doubly distilled water (resistivity 18.2 $\text{M}\Omega$ at 25° C) was used to prepare all solutions. A phosphate buffer solution (PBS) was prepared by mixing 0.1 M sodium phosphate dibasic and 0.1 M sodium phosphate monobasic. The Acetate buffer solution was prepared by mixing 0.1 M sodium acetate (0.1 M) and acetic acid (0.1 M). The pH meter adjusted the supporting electrolyte pH by adding 0.1 M HCl and 0.1 M NaOH.

Text S2. Instrumentation

Field emission-scanning electron microscope (FE-SEM) was used for the surface morphology (Nova Nano SEM 450, FEI, USA), and X-ray diffractometer (XRD) analysis (X'Pert PRO, PANalytical, Netherland) was done in the range of 20°-60° with a step size of 0.02° using $\text{CuK}\alpha$ radiation of 1.54 Å wavelength to acquire the structural information. The Brunauer- Emmett-Teller (BET) method (NOVATouch LX2, Quantachrome, USA) confirmed the porous structure. The Fourier Transform Infra-red (FT-IR) (Shimadzu, Kyoto, Japan) was done to know the functional group in the nanocomposite in the 4000 cm^{-1} –500 cm^{-1} , taken in the KBr mode. A Raman spectrometer (STR-MPR 500-Micro, Technos, India) employing an Ar ion laser at 532 nm was used. The high-resolution transmission electron microscope (HR-TEM, Tecnai G2 20 (FEI)) sample was prepared by dispersing the nanocomposite in isopropanol, ultrasonication, and then drop-casting onto the copper grid.

All the electrochemical studies were done in the cell, consisting of the three-electrode system with Pt wire as the counter electrode, Glassy carbon electrode (GCE) as the working electrode, and Ag/AgCl as the reference electrode. Cyclic voltammetry (CV) and differential pulse voltammetry (DPV) were

studied on the Klyte electrochemical workstation using the software PG-Lyte 1.0.5.2. Electrochemical impedance spectroscopy (EIS) study was performed on the potentiostat (SP-150, BioLogic, France) with an amplitude of 5 mV in the frequency range of 0.01 – 100 Hz, and Randle 's-sevcik fitting curve was obtained using software EC lab v11.30.

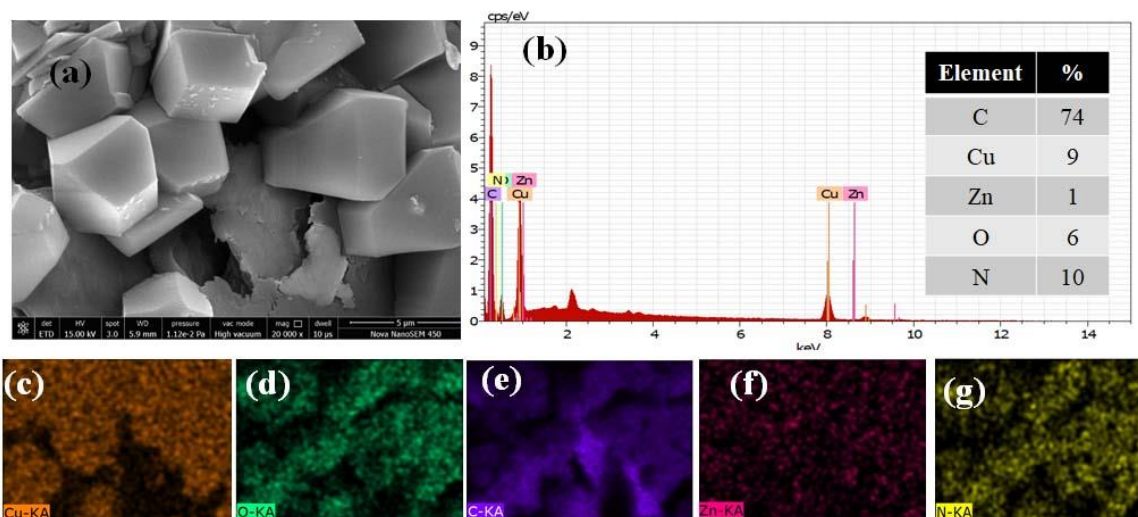


Fig. S1. (a)FE-SEM image of Zn-Cu MOF/rGO, (b) Energy-dispersive spectroscopy (EDS) spectrum of Zn-Cu MOF/rGO, (c) elemental mapping image of copper, (d) elemental mapping image of oxygen, (e) elemental mapping image of carbon, (f) elemental mapping image of zinc, and (d) elemental mapping image of nitrogen.

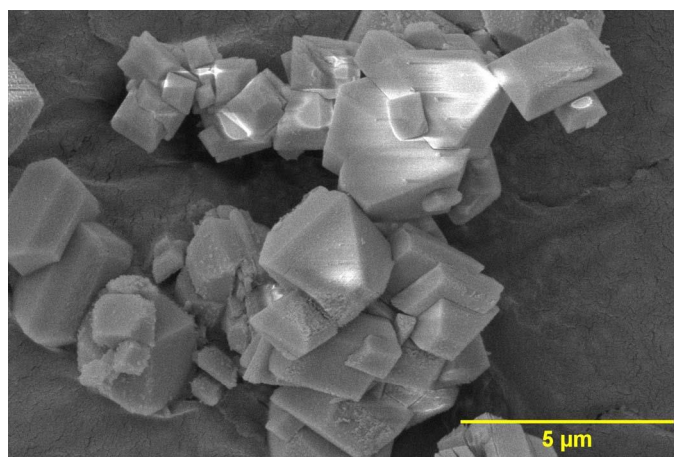


Fig. S2. FE-SEM image of Zn-Cu MOF

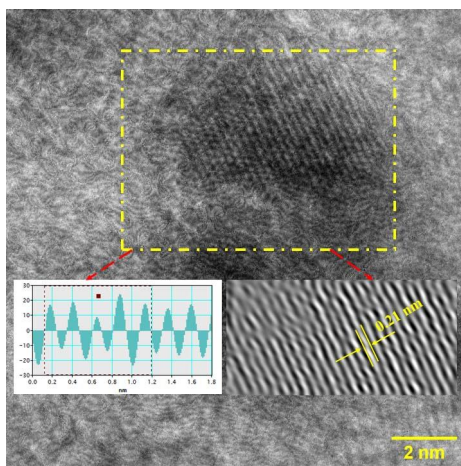


Fig. S3 Interlayer plane of the Zn-Cu MOF/rGO nanocomposite

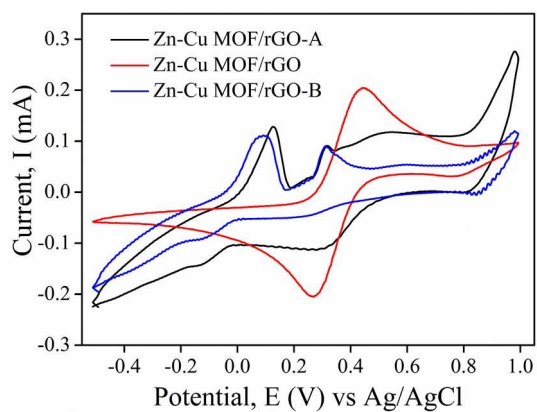


Fig. S4. Comparative CV of Zn-Cu MOF/rGO-A, Zn-Cu MOF/rGO, and Zn-Cu MOF/rGO-B recorded in the 10 mM $K_3[Fe(CN)_6]/K_4[Fe(CN)_6]$ + 0.1 M KCl at the scan rate of 50 mV/s.

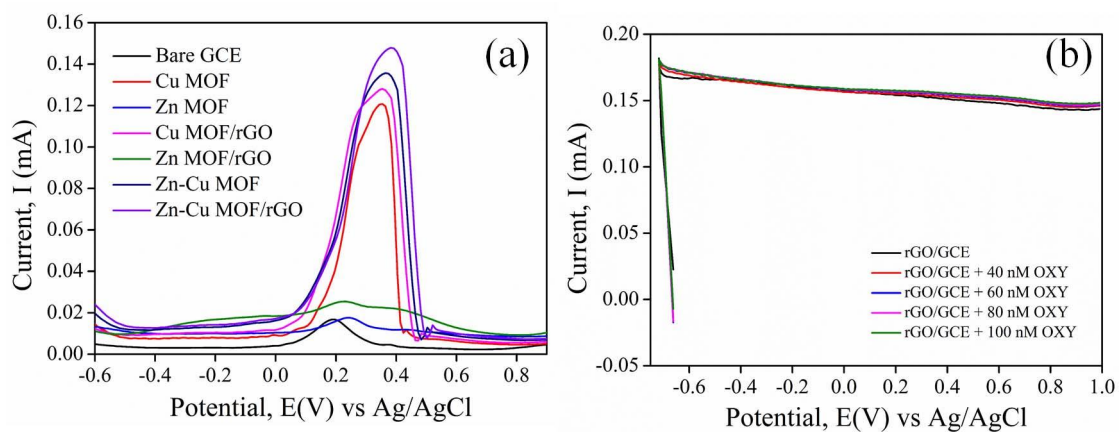


Fig. S5. (a) DPV curve recorded for the bare GCE, Cu MOF, Zn MOF, Cu MOF/rGO, Zn MOF/rGO, Zn-Cu MOF, Zn-Cu MOF/rGO, (b) DPV curve recorded for the rGO modified GCE without and with different concentrations of OXY (Supporting electrolyte: 0.1 M ABS, pH 5).

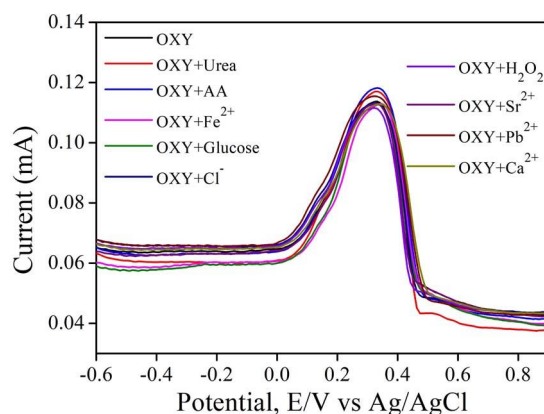


Fig. S6. DPV response curve for Zn-Cu MOF/rGO/GCE in the presence of OXY and other analyte presence (0.1 M ABS, pH 5).

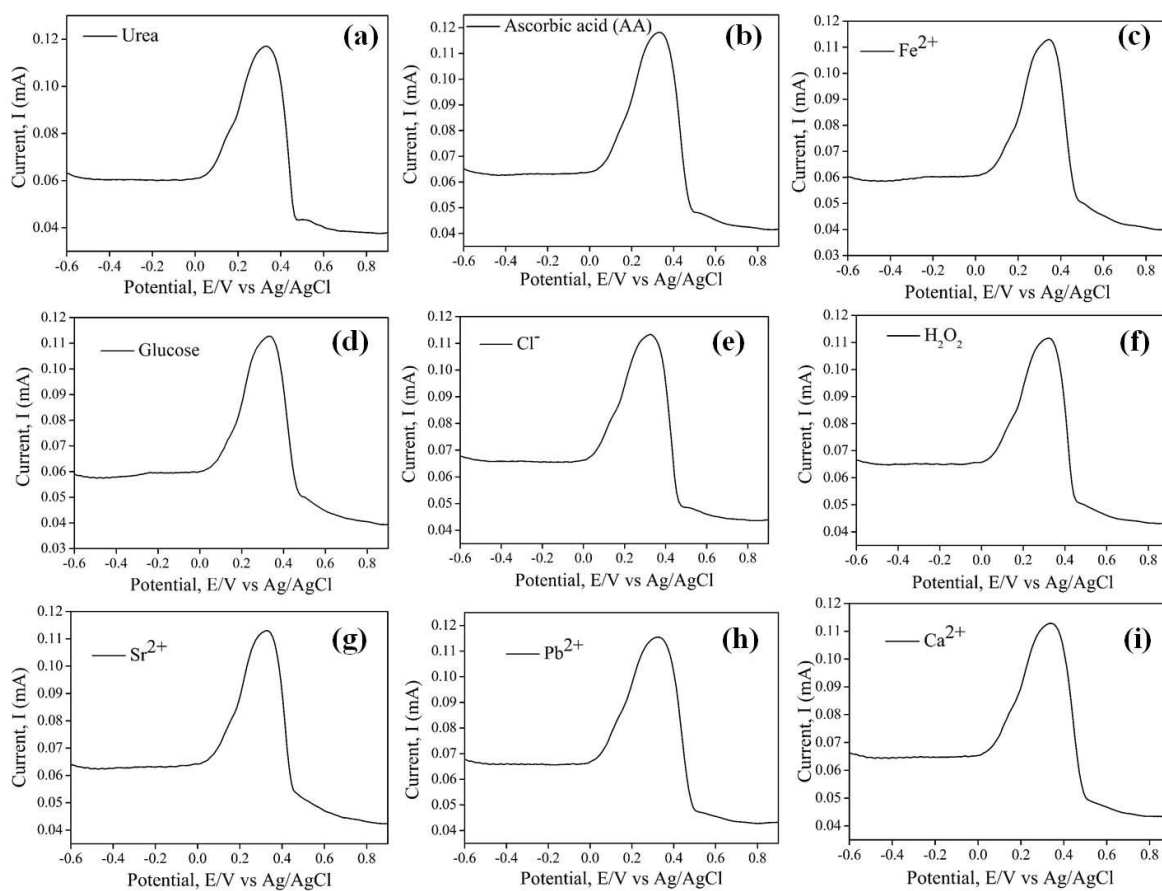


Fig. S7. DPV response curve for Zn-Cu MOF/rGO/GCE in the presence of different analytes, (a) 100 nM Urea, (b) 100 nM Ascorbic acid (AA), (c) 100 nM Fe²⁺, (d) 100 nM Glucose, (e) 100 nM Cl⁻, (f) 100 nM H₂O₂, (g) 100 nM Sr²⁺, (h) 100 nM Pb²⁺, (i) 100 nM Ca²⁺ (0.1 M ABS, pH 5).

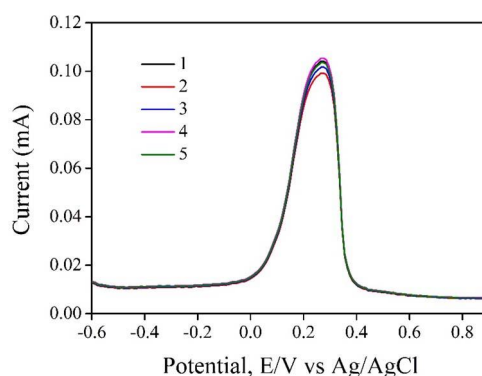


Fig. S8. DPV curve for the Zn-Cu MOF/rGO/GCE for the five different electrode

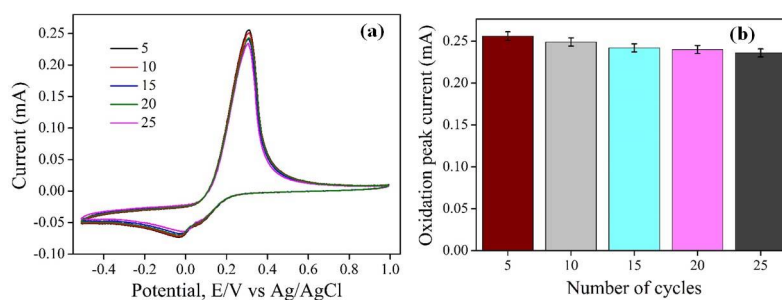


Fig. S9. (a) CV curve for the different number of cycles for stability study, (b) corresponding current variation.

Table S1. Parameters for the synthesis of composite material using a one-pot solvothermal approach

Material	Composition	Solvent	Temperature (°C)	Time (h)
Zn MOF	Zn(NO ₃) ₂ ·6H ₂ O, terephthalic acid	30 mL DMF 30 mL ethanol	85	20
Cu MOF	Cu(NO ₃) ₂ ·3H ₂ O, terephthalic acid	30 mL DMF 30 mL ethanol	85	20
Zn MOF/rGO	Zn(NO ₃) ₂ ·6H ₂ O, terephthalic acid, 5 wt% rGO	30 mL DMF 30 mL ethanol	85	20
Cu MOF/rGO	Cu(NO ₃) ₂ ·3H ₂ O, terephthalic acid, 5 wt% rGO	30 mL DMF 30 mL ethanol	85	20

Table S2. Electrochemical properties for the different electrodes

Electrode	Anodic peak Current (mA)	Active surface area (cm²)
Bare GCE	0.098	0.060
Zn MOF/GCE	0.0035	0.002
Zn MOF/rGo/GCE	0.0055	0.0035
Cu MOF/GCE	0.051	0.032
Cu MOF/rGO/GCE	0.025	0.016
Zn-Cu MOF/GCE	0.057	0.035
Zn-Cu MOF/rGO-A/GCE	0.128	0.080
Zn-Cu MOF/rGO-B/GCE	0.095	0.059
Zn-Cu MOF/rGO/GCE	0.205	0.127

Table S3: List of the oxidation peak current for the different materials modified on GCE in 0.1 M ABS (pH 5)

Material	Oxidation peak potential (V)	Oxidation peak current (mA)
Bare GCE	0.211	0.008
Zn MOF/GCE	0.251	0.012
Zn MOF/rGO/GCE	0.257	0.048
Cu MOF/GCE	0.365	0.208
Cu MOF/rGO/GCE	0.399	0.246
Zn-Cu MOF/GCE	0.397	0.258
Zn-Cu MOF/rGO/GCE	0.330	0.314